EVALUATION OF SOIL-STRUCTURE INTERACTION EFFECTS FROM STRONG MOTION RECORDINGS

J. P. Stewart
Department of Civil & Environmental Engineering
University of California, Los Angeles

ABSTRACT

This paper reviews the results of recent studies that have investigated the effects of soil-structure interaction (SSI) on the seismic response of building structures using recorded strong motions. Two manifestations of SSI are described: (1) inertial interaction effects on the effective first-mode period and damping ratio of buildings, and (2) variations between foundation-level and free-field ground motions. Inertial interaction effects are seen to increase with the ratio of soil-to-structure stiffness, and are reasonably well predicted with simplified analytical formulations similar to those in the NEHRP Provisions (BSSC, 1997). Ground motions in structures are seen to generally be less than free-field motions. Foundation embedment and frequency are shown to significantly affect the variations between these motions.

INTRODUCTION

Documentation of seismic case history data is a critically important step towards understanding and reliably characterizing complex problems in geotechnical earthquake engineering. Few empirical studies of soil-structure interaction (SSI) have been previously performed, although the literature on analytical procedures for SSI is extensive.

This paper is a summary of some previous and ongoing work at UCLA that is seeking to document SSI effects from strong motion recordings. The paper is divided into two main sections. The first section reviews inertial interaction effects on structural response. These effects are quantified in terms of the ratio of flexible- to fixed-base first mode period $\tilde{T}/T$ and foundation damping factor $\tilde{\zeta}_0 = \tilde{\zeta} - \zeta/(\tilde{T}/T)^3$, where ζ and $\tilde{\zeta}$ = fixed- and flexible-base first mode damping ratio, respectively. The subject of the second section is foundation/free-field ground motion variations that result from kinematic interaction (embedment, base-slab averaging) and inertial interaction.

INERTIAL INTERACTION EFFECTS ON FIRST-MODE VIBRATION PARAMETERS

Evaluation of Modal Parameters from Strong Motions Recordings

Three cases of base fixity are of interest in analyses of SSI: (1) fixed-base, representing only the flexibility of the structure, (2) flexible-base, representing the combined flexibility of the

complete soil-structure system, and (3) pseudo flexible-base, representing flexibility in the structure and rocking in the foundation. Pseudo flexible-base parameters are of interest because they can sometimes be used to approximate flexible-base parameters or to estimate either fixed- or flexible-base parameters.

Stewart and Fenves (1998) evaluated the types of input and output strong motion recordings that should be used in system identification analyses to evaluate fixed-, flexible- and pseudo flexible-base vibration parameters of structures. While roof translations are always used as output, the input motions for various base fixity conditions vary as indicated in Fig. 1. Recordings of free-field, foundation, and roof-level translations, as well as base rocking, are needed to evaluate directly both fixed- and flexible-base modal parameters of a structure. The system identification procedures used to evaluate modal parameters for a given input and output are described by Stewart and Fenves (1998).

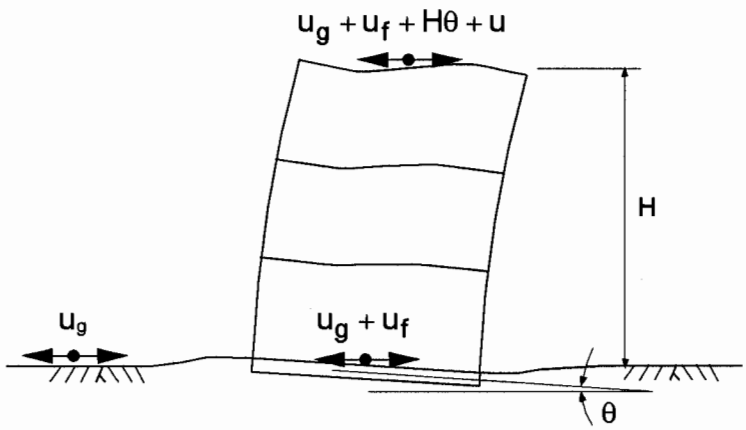

Fig. 1: Input and output motions for system identification

Instrumented building sites often lack sensors for recording base rocking or free-field translations. For such cases either fixed-base parameters (missing base rocking) or flexible-base parameters (missing free-field translations) cannot be evaluated directly from system identification analyses. Stewart and Fenves (1998) derived expressions to estimate either flexible- or fixed-base parameters using "known" modal parameters for the two other cases of base fixity. The estimation procedures operate on the premise that differences between known parameters can be used to calibrate the foundation impedance at the structure's period; the calibrated impedance can then be used to estimate the unknown parameters. These estimation procedures extend significantly the number of sites for which SSI effects can be empirically evaluated.

Database

Two classes of sites are considered: Class 'A' sites, which have a free-field accelerograph and a structure instrumented to record base and roof translations (and in some cases, base rocking as well), and Class 'B' sites, which have structures instrumented to record base rocking as well as base and roof translations, but have no free-field accelerographs. Criteria employed in the selection of 'A' sites are described by Stewart et al. (1999a).

Suitable free-field instruments were sought for virtually all instrumented structures in California, and 44 sites were identified (plus one additional structure in Taiwan). An additional 13 structures in California were considered in this study as 'B' sites. For the 57 sites, 74 processed data sets are available as a result of multiple earthquake recordings at 13 sites. Fifteen California earthquakes contributed data to this study with magnitudes ranging from 4.8 to 7.3. Moderate to low level shaking (pga < 0.1 to 0.2g) is well represented in the database (50 data sets), while a moderate amount of data (24 data sets) is available for more intense shaking (pga > 0.2g). The foundation conditions at the sites include 23 buildings with piles or piers, and 34 with footings, mats, or grade beams. Most buildings are not embedded (36) or have shallow single-level basements (14). Only seven buildings have multi-level basements. The buildings range from single story warehouses to high-rise office buildings. Lateral force resisting systems include shear walls, frames, and base isolation.

Evaluation of Period Lengthening and Foundation Damping

Period lengthening ratios and foundation damping factors derived from fixed- and flexible-base modal vibration parameters obtained from system identification analyses are shown in Fig. 2. These parameters are plotted against the dimensionless structure-to-soil stiffness ratio $1/\sigma = h/(V_S \cdot T)$, where h = effective structure height and V_S = effective soil shear wave velocity. Also shown are second-order polynomials fit to the data by regression analysis, and analytical results by Veletsos and Nair (1975) for h/r = 1 and 2 (where r = foundation radius). Both $\tilde{T}/T$ and $\tilde{\zeta}_0$ are seen to increase with $1/\sigma$, and the best fit lines through the data are similar to the Veletsos and Nair curves.

There is significant scatter in the data in Fig. 2, although much of this results from systematic variations in $\tilde{T}/T$ and $\tilde{\zeta}_0$ associated with factors such as structure aspect ratio, embedment, foundation type, and foundation shape and flexibility effects. In addition, $\tilde{\zeta}_0$ is influenced by the hysteretic soil damping (β), which varies with soil type.

Results from several sites help to illustrate the strong influence of $1/\sigma$ on inertial interaction effects. The most significant inertial interaction occurred at site A46 ($\tilde{T}/T \approx 4$ and $\tilde{\zeta}_0 \approx 30\%$), which has a stiff ($T \approx 0.1$ sec) cylindrical concrete structure (h=14.3 m) and relatively soft soils ($V_S \approx 85$ m/s), giving a large $1/\sigma$ of about 1.5. Conversely, the inertial interaction effects are negligible at site A21 ($\tilde{T}/T \approx 1$ and $\tilde{\zeta}_0 \approx 0\%$), which has a relatively flexible ($T \approx 0.8$-1.0 sec) base-isolated structure (h=6.7 m) that is founded on rock ($V_S \approx 300$ m/s), giving a much smaller $1/\sigma$ value of 0.02-0.03. These two sites represent the extremes of inertial interaction. More typical SSI effects occur at sites B14 ($\tilde{T}/T = 1.14$ and $\tilde{\zeta}_0 \approx 3.4\%$) and A1-tr ($\tilde{T}/T = 1.57$ and $\tilde{\zeta}_0 \approx 15.4\%$). The structures at both sites are shear wall buildings with periods of T = 0.49 and 0.15 sec, respectively, and are founded on medium-stiff soils (V_S = 256 and 213 m/s), combining to give $1/\sigma \approx 0.12$ at B14 and $1/\sigma \approx 0.29$ at A1-tr. The results from these four sites illustrate that both $\tilde{T}/T$ and $\tilde{\zeta}_0$ increase with increasing $1/\sigma$.

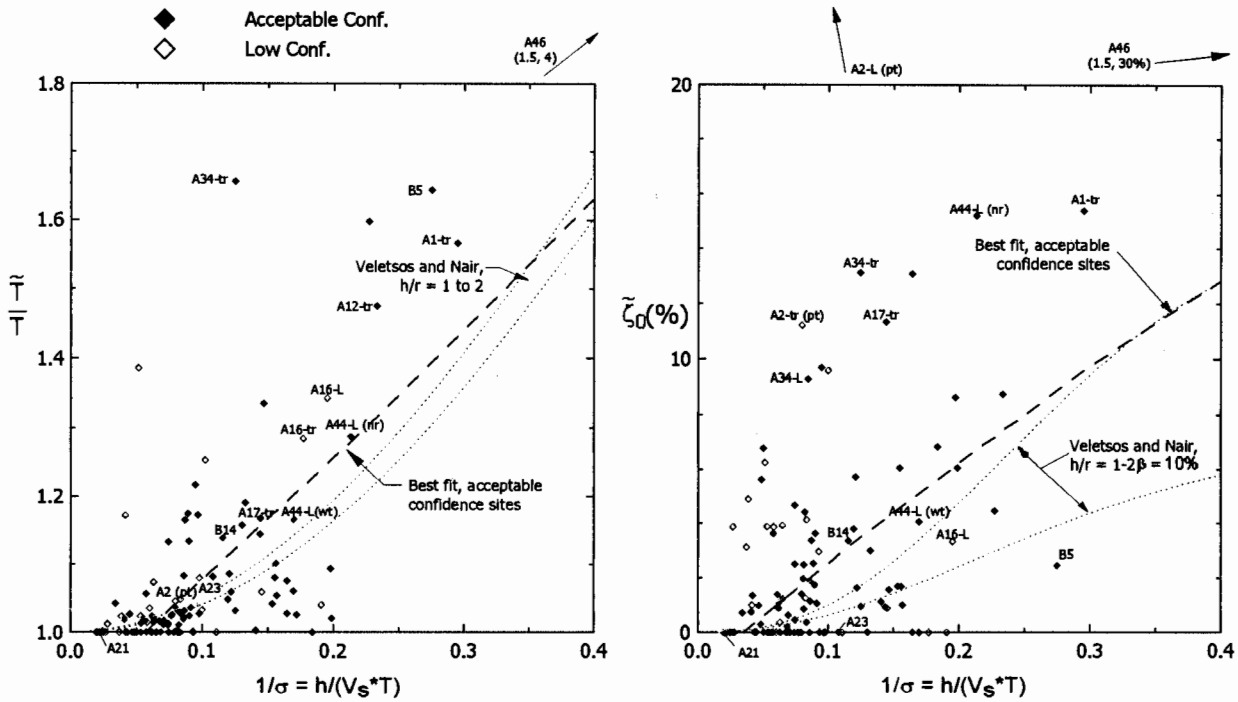

Fig. 2: Period lengthening ratios and foundation damping factors for sites sorted by confidence level (tr=transverse, L = longitudinal)

Comparison to Analysis

For analysis of inertial interaction effects, the objectives are predictions of first-mode period lengthening ratio $\tilde{T}/T$ and foundation damping factor $\tilde{\zeta}_0$. As shown in Fig. 3, simple procedures for evaluating these effects employ a model consisting of a single degree-of-freedom structure resting on a foundation-soil system represented by an impedance function. The impedance function is calculated for a rigid disk foundation resting either at the surface of (Veletsos and Nair, 1975) or embedded into (Bielak, 1975) a uniform visco-elastic halfspace.

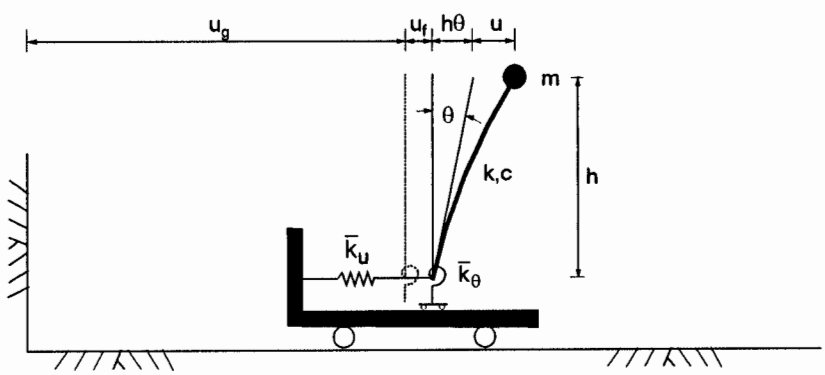

Fig. 3: Simplified model for analysis of inertial interaction

The foundation impedance function is evaluated at the flexible-base period of the structure, $\tilde{T}$. The frequency dependent and complex-valued impedance terms are expressed in the form

$$\bar{k}_j = k_j(a_0, \upsilon) + i\omega c_j(a_0, \upsilon) \tag{1}$$

where j denotes either deformation mode u (translation) or θ (rocking), ω is angular frequency (radians/sec.), a_0 is a dimensionless frequency defined by $a_0 = \omega r/V_S$, r = foundation radius, and υ = soil Poisson ratio. Terms k_j and c_j consist of a combination of static foundation stiffness (K_j) and dynamic modifiers α_j and β_j as follows:

$$k_j = \alpha_j K_j \qquad\qquad c_j = \beta_j \frac{K_j r}{V_s} \tag{2}$$

The terms α_j and β_j express the frequency dependence of the impedance, and are computed differently for surface (Veletsos and Verbic, 1973) and embedded (Bielak, 1975) foundations. Foundation radii are computed separately for translational and rotational deformation modes to match the area (A_f) and moment of inertia (I_f) of the actual foundation (i.e. $r_u = \sqrt{A_f/\pi}$, $r_\theta = \sqrt[4]{4I_f/\pi}$). The Bielak formulation includes a rigorous model of dynamic basement wall-soil interaction, assuming perfect wall-soil bonding. An approximate analysis of embedment effects can be made with the Veletsos and Nair model by increasing the static stiffness according to the well known guidelines of Kausel (1974), and using α_j and β_j terms for surface foundations (Elsabee and Moray, 1977).

Stewart et al. (1999a) outlined several considerations associated with the application of these procedures to realistic foundation and soil conditions. These can be summarized as follows:

1. *Representation of nonlinear soil response and nonuniform soil profiles as a visco-elastic halfspace*. Strain dependent soil properties are evaluated here with site response analyses which are used to calculate an equivalent hysteretic damping ratio and a degraded shear wave velocity profile. The effective profile velocity is taken as the profile depth divided by the shear wave travel time through the degraded profile. Profile depth is taken as $r_u = \sqrt{A_f/\pi}$.

2. *Representation of non-circular foundations*. While noncircular foundations with aspect ratios < 4:1 can generally be represented as equivalent disks (Roesset, 1980), radiation dashpot coefficients for rocking can be underestimated by such procedures (Dobry and Gazetas, 1986). Correction factors can be adapted from the Dobry and Gazetas results.

3. *Representation of flexible foundations*. The impedance of flexible base mats with thin perimeter walls or rigid concentric interior and perimeter walls can be reasonable well represented by rigid foundation models (Liou and Huang, 1994; Riggs and Waas, 1985). However, the rigid disk model is inadequate for buildings with rigid central cores, and should be modified according to the results of Iguchi and Luco (1982).

The basic procedures for a rigid disk foundation on the surface of, or embedded into, a halfspace were modified according to (1) to (3) above, and are subsequently referred to as the "modified Veletsos" (MV) and "modified Bielak" (MB) formulations.

Period lengthening ratios and foundation damping factors were evaluated by the Modified Veletsos (MV) procedure. For embedded foundations, similar comparisons using the Modified Bielak (MB) procedure are described by Stewart et al. (1999b).

Deviations in MV predictions of $\tilde{T}/T$ and $\tilde{\zeta}_0$ relative to empirical values are shown in Fig. 4 for sites with acceptable and low confidence designations. Also plotted are best fit second-order polynomials established from regression analyses on data from acceptable confidence sites. For most sites, the predictions are accurate to within absolute errors of about ±0.1 in $\tilde{T}/T$ and ±3% damping in $\tilde{\zeta}_0$ for $1/\sigma = 0$ to 0.4. The regression curves indicate no significant systematic bias in predictions of either $\tilde{T}/T$ or $\tilde{\zeta}_0$ up to $1/\sigma = 0.4$. However, there is a downward trend in the best fit curve for damping for $1/\sigma > 0.5$ (beyond the range on Fig. 4) due to a significant underprediction of $\tilde{\zeta}_0$ at site A46 ($1/\sigma = 1.5$) which results from a pronounced embedment effect at this site that is not fully captured by the MV formulation.

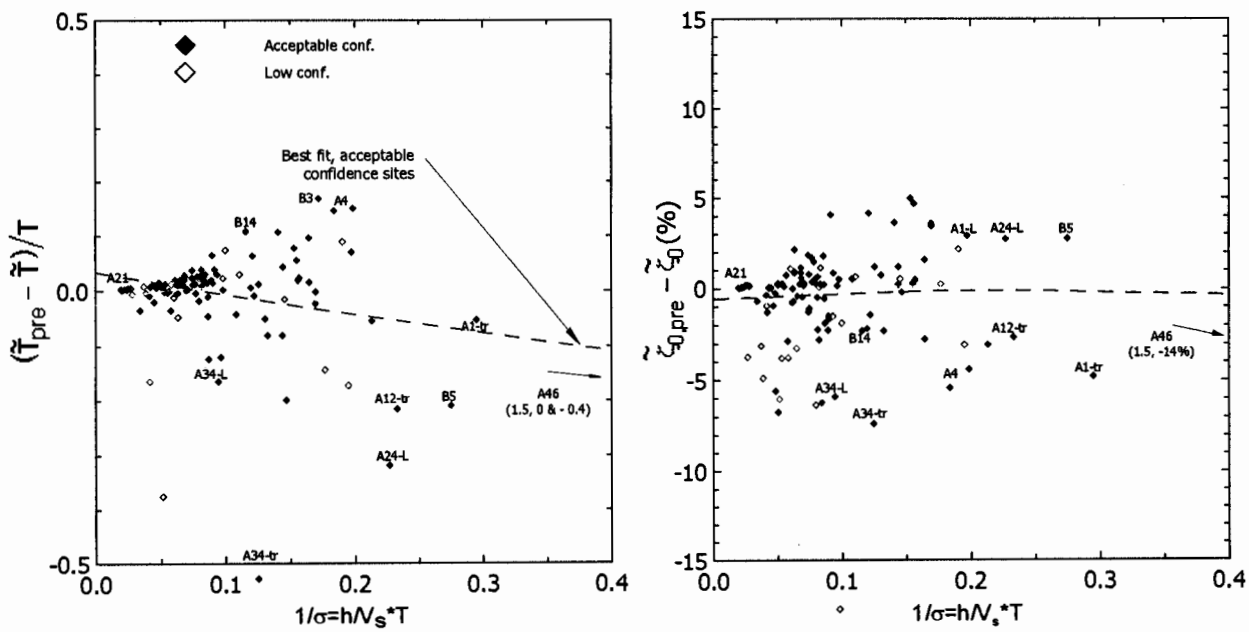

Fig. 4: Errors in "modified Veletsos" formulation for sites sorted by confidence level

The results from several sites help illustrate the general findings of Fig. 4. The minimal inertial interaction effects at site A21 ($1/\sigma = 0.02$ to 0.03, $\tilde{T}/T \approx 1$ and $\tilde{\zeta}_0 \approx 0\%$) are well predicted by the MV analyses, as is typical for sites with $1/\sigma < 0.1$. The predictions are also generally satisfactory for sites with intermediate $1/\sigma$ values such as B14 and A1-tr ($1/\sigma = 0.12$, $1/\sigma = 0.29$). At these sites, period lengthenings of 1.14 and 1.57 are over- and under-predicted by

absolute differences of about 0.11 and 0.06, respectively, while foundation damping factors of 3.4 and 15.4% are underpredicted by absolute differences of 2.3 and 4.8%, respectively. The large inertial interaction effects at site A46 ($1/\sigma = 1.5$, $\tilde{T}/T \approx 4.0$ and $\tilde{\zeta}_0 \approx 30\%$) are predicted to within an absolute difference of about 0.4 for period lengthening, but damping is underpredicted by an absolute difference of about 14%. With the exception of the damping results at site A46 (where there is a significant embedment effect), these results indicate that predictions of $\tilde{T}/T$ and $\tilde{\zeta}_0$ by the MV procedure are reasonably good considering the breadth of conditions represented in the database.

There are several noteworthy outliers in Fig. 4. When the residuals in Fig. 4 are considered with respect to the magnitude of the observed SSI effect, the most significant outliers for period lengthening are seen to be site A34 and several long period structures (A4, B3). The unusual results at site A34 may be associated with erroneously high shear wave velocity measurements. The long period structures at sites A4 and B3 are founded on soft Bay Mud soils in the San Francisco Bay Area, and were subject to negligible period lengthening (a common system identification result for all long-period structures). The soft soils at sites A4 and B3 lead to overpredictions of period lengthening, suggesting an error in the model. It appears from these data that the simple single-degree-of-freedom models on which the MV and MB formulations are based are incapable of adequately modeling SSI effects in long period structures with significant higher mode responses.

VARIATIONS BETWEEN FOUNDATION AND FREE-FIELD GROUND MOTIONS

It is widely known that soil-structure interaction modifies foundation-level motions relative to free-field motions (Kramer, 1996; Chopra, 1995), with both amplification and de-amplification of foundation-level motion possible across different frequency ranges. Two mechanisms of SSI generate the deviations between foundation and free-field motions:

- *Inertial Interaction*: Inertia developed in the structure due to its own vibrations gives rise to base shear and moment, which in turn causes displacements and rocking of the foundation relative to the free-field. These relative displacements can lead to amplification of foundation-level motion relative to the free-field at the fundamental-mode period of the structure ($\tilde{T}$).
- *Kinematic Interaction*: An assemblage of stiff foundation elements located on or in soil moves as a constrained body. Since free-field motions are generally spatially and temporally incoherent, motions on surface foundations are typically filtered with respect to free-field motions through a process termed "base slab averaging" by Seed (1986). Embedded foundations are subject to additional ground motion filtering associated with the reduction of ground motion amplitude with depth. Kinematic effects are most pronounced at high frequencies.

At a site with recordings of both free-field and foundation-level motions, variations between these motions result from a composite of kinematic and inertial effects, as well as random variations resulting from spatial incoherence effects.

Fig. 5 compares maximum horizontal acceleration (MHA) and spectral acceleration at the first-mode building period ($S_a@\tilde{T}$) for a data set consisting of 'A' sites in the aforementioned database (both transverse and longitudinal data are included). The MHA data in Fig. 5 generally indicate de-amplification of foundation-level MHA, and a perceptible increase in the level of de-amplification with increasing MHA. Filtering of foundation motion is significantly smaller in the $S_a@\tilde{T}$ data. The MHA de-amplification reflects the significant influence of kinematic interaction at high frequencies. The relatively modest de-amplification of $S_a@\tilde{T}$ results from both foundation motion amplification associated with inertial interaction, which is most pronounced at $\tilde{T}$, and the reduced kinematic effect at longer spectral periods.

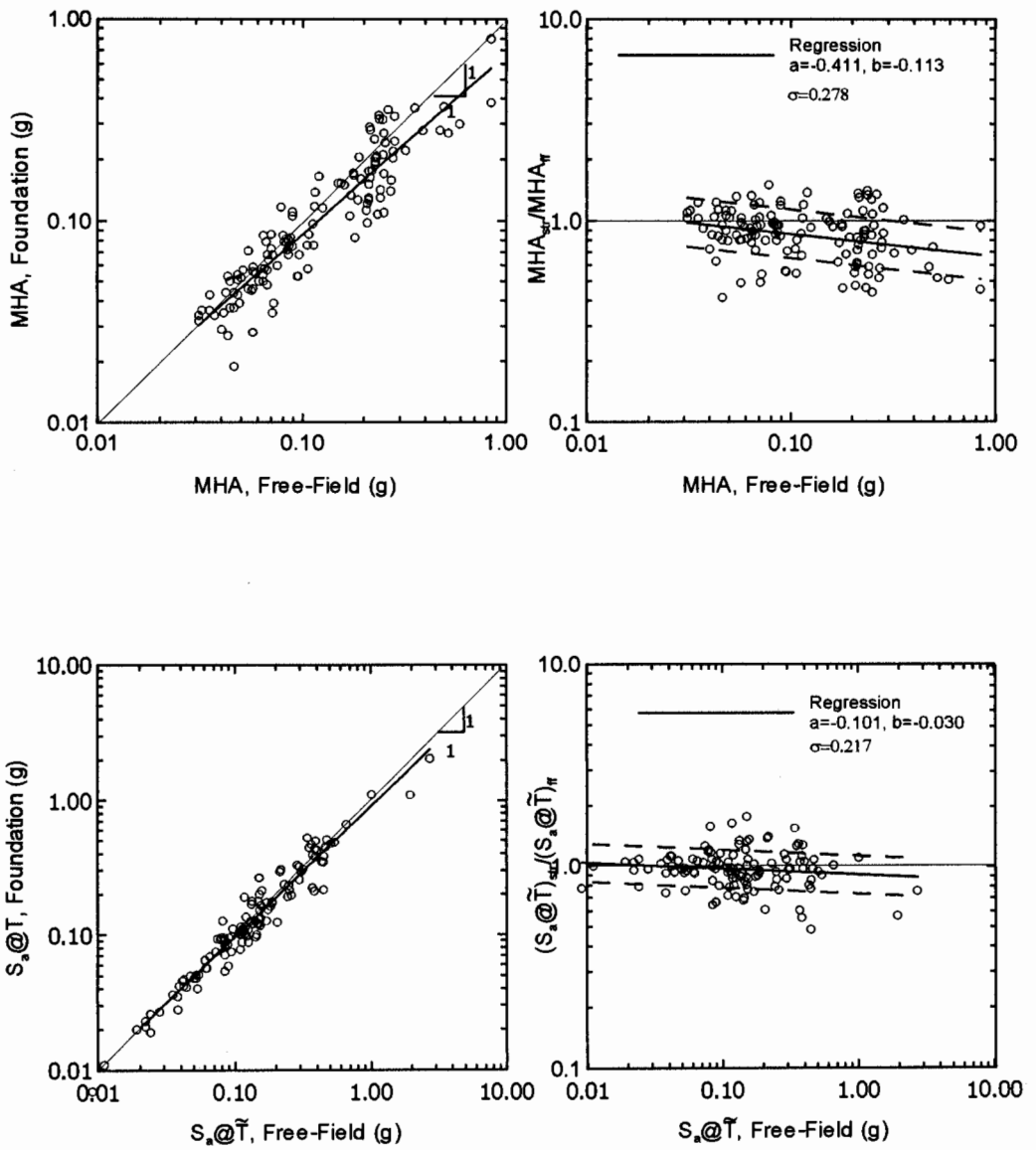

Fig. 5: Variation between free-field and foundation-level MHA and 5% damped $S_a@\tilde{T}$, full data set

In order to elucidate trends in the data plotted in Fig. 5, linear regression analyses were performed to fit an equation of the following form to the data,

$$\ln(ratio) = a + b\ln(ff) \tag{3}$$

where *ratio* is the ratio of foundation/free-field motion and *ff* is the amplitude of the free-field motion. The result of this regression is plotted in Fig. 5. More complex equation forms were investigated, but did not significantly reduce residuals. The residuals between the data and regression results are essentially log-normally distributed. Accordingly, the standard error of the regression, denoted henceforth as σ, is computed from the log of the residuals, with the results listed in Fig. 5. Regression results $\pm\ \sigma$ are plotted in Fig. 5 as dashed lines. It may be noted that the error term for MHA (σ=0.278) significantly exceeds that for $S_a@\tilde{T}$ (σ=0.217), suggesting a higher level of data noise at high frequencies where spatial incoherence effects are most pronounced.

Elsabee and Morray (1977) and Day (1978) found from finite element analyses of cyclindrical embedded foundations that embedement ratio (*e/r*) is a significant parameter controlling the filtering of embedded foundation-level motion relative to free-field motion. Fig. 6 compares ratios of MHA and $S_a@\tilde{T}$ data for the full data set sorted according to *e/r* = 0, *e/r* > 0 & < 0.5, and *e/r* > 0.5. Also plotted in Fig. 6 are regression results fitting Eq. 3 for the different data bins. The $S_a@\tilde{T}$ data for *e/r* > 0 & < 0.5 has negligible deviations from the *e/r* = 0 data. The MHA deviations for these two *e/r* bins are larger, but are still modest. Although the data for *e/r* > 0.5 is sparse, significant and consistent de-amplification is apparent both in MHA and $S_a@\tilde{T}$ relative to *e/r* < 0.5. Therefore, it appears that *e/r* is an important index controlling foundation/free-field ground motion variations.

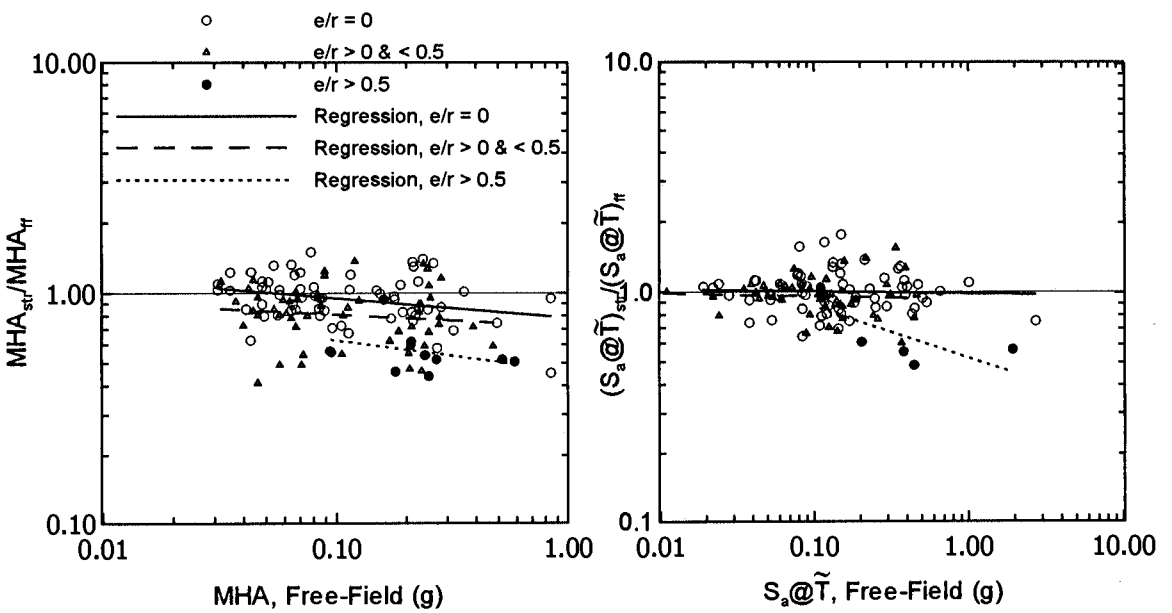

Fig. 6: Ratio of foundation-level/free-field motion, complete data set, sorted by e/r

As noted previously, inertial interaction effects in buildings are strongly a function of $1/\sigma$. Data from sites with $e/r < 0.5$ are sorted into bins with $1/\sigma < 0.1$ and $1/\sigma > 0.1$ and are plotted in Fig. 7 along with regressions according to Eq. 1. The results indicate that motions in buildings with $1/\sigma > 0.1$ are larger than motions with negligible inertial interaction. This suggests that structural vibrations enhance foundation-level motions in buildings with significant inertial interaction, which is expected. However, the inertial interaction effect on foundation-level ground motions is fairly small.

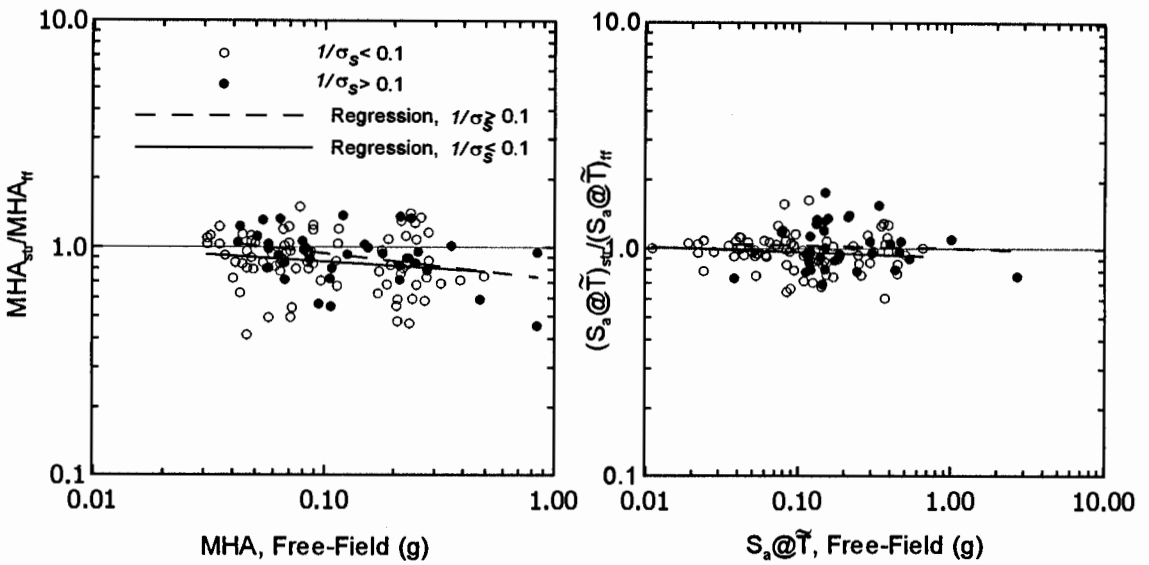

Fig. 7: Ratio of foundation-level/free-field motion, data set with e/r < 0.5, sorted according to $1/\sigma < 0.1$ and $1/\sigma > 0.1$

Veletsos and Prasad (1989) and Veletsos et al. (1997) investigated with theoretical analysis base slab averaging effects for rigid foundations subjected to nonvertically incident and incoherent wave fields. It was found that the filtering of translational motion on base slabs increases with dimensionless frequency, $\tilde{a}_0$, defined for circular foundations as,

$$\tilde{a}_0 = \frac{\omega r}{V_s}\sqrt{\kappa^2 + \sin^2 \alpha_v} \qquad (4)$$

where κ=an incoherence parameter for the incident waves which varies between 0 and 1.0, and α_v=vertical angle of incidence of waves. Stewart (1999) found a strong effect of $\tilde{a}_0$ on foundation/free-field ground motion ratios at various spectral frequencies (ω), but the effect was traced principally to ω (i.e. variations with $\tilde{a}_0/\omega$ were negligible). Accordingly, base slab averaging effects can be grossly approximated using single median values of spectral acceleration ratio and standard error terms evaluated across a range of spectral periods (T=0.18, 0.32, 0.56, 1.0, 1.8, and 3.0 s) using data with $e/r < 0.5$. The results are compiled in Fig. 8, and show decreasing bias and standard error with increasing spectral period up to $T \approx 0.5$ s. These results

suggest that for $T \geq \sim 0.5$ s, median foundation-level spectral accelerations are within about 5 percent of free-field spectral accelerations, and that the standard error of the ratio is small ($\sigma \approx$ 0.18 to 0.22). This finding is consistent with Campbell (1984), who also found negligible de-amplification for spectral periods larger than 1 s.

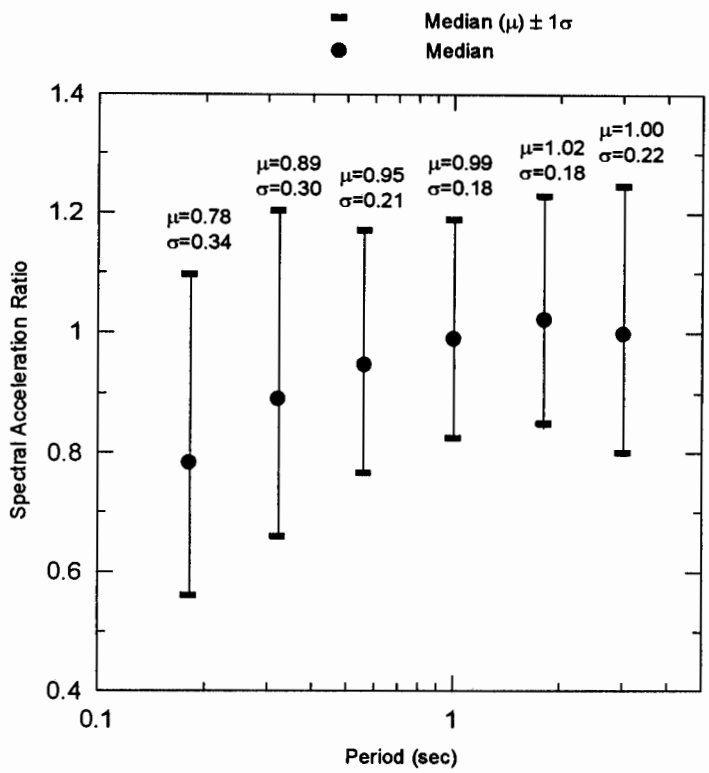

Fig. 8: Statistical values of 5% damped spectral acceleration ratio for various spectral periods, data set with $e/r < 0.5$

CONCLUSIONS

Based on the database of 57 sites compiled for this study, the factor with the greatest influence on $\widetilde{T}/T$ and $\widetilde{\zeta}_0$ is the ratio of structure-to-soil stiffness as quantified by the parameter $1/\sigma = h/(V_S \cdot T)$. When $1/\sigma$ is nearly zero, $\widetilde{T}/T$ and $\widetilde{\zeta}_0$ values are about unity and zero, respectively, whereas at the maximum observed value of $1/\sigma = 1.5$ at site A46, interaction effects dominated the structural response ($\widetilde{T}/T \approx 4$ and $\widetilde{\zeta}_0 \approx 30\%$). Additional factors which can significantly affect inertial interaction include the structure's aspect ratio (h/r) and foundation embedment and flexibility.

Variations between foundation and free-field motions result from kinematic and inertial soil-structure interaction effects. While inertial interaction can lead to minor amplification of foundation motion relative to the free-field, kinematic effects, which de-amplify high frequency motions, are generally more significant.

ACKNOWLEDGMENTS

Support for this work was provided by a CAREER award from the National Science Foundation (Award No. CMS 9733113). The views and conclusions contained in this document are those of the author and should not be interpreted as necessarily representing the official policies, either expressed or implied, of the U.S. Government.

REFERENCES

Bielak, J. (1975). "Dynamic behavior of structures with embedded foundations," *J. Eq. Engrg. Struct. Dynamics*, 3(3), 259-274.

Building Seismic Safety Council, BSSC (1997). "NEHRP Recommended provisions for seismic regulations for new buildings and other structures, Part 1, Provisions and Part 2, Commentary" *Rpt. No. FEMA 302*, Federal Emergency Management Agency, Washington D.C.

Campbell, K.W. (1984). "Near-source attenuation of strong ground motion for moderate to large earthquakes—An update and suggested application for the Wasatch Fault Zone of Norhcentral Utah," *in* Evaluation of Regional and Urban Earthquake Hazards and Risk in Utah, W.W. Hays and P.L. Gori (eds.), Proc. 26th NEHRP Workshop, Salt Lake City, Utah, Rpt. No. USGS OFR 84-763.

Chopra, A.K. (1995). *Dynamics of Structures.* Prentice Hall, Upper Saddle River, NJ, pg. 192.

Day, S.M. (1978). "Seismic response of embedded foundations," *Proc. ASCE Convention*, Chicago, IL, October, Preprint 3450.

Dobry, R. and Gazetas, G (1986). "Dynamic response of arbitrarily shaped foundations," *J. Geotech. Engrg.*, ASCE, 112(2), 109-135.

Elsabee, F. and Morray, J.P. (1977). "Dynamic behavior of embedded foundations," *Rpt. No. R77-33*, Dept. of Civil Engrg., Massachusetts Inst. Technology.

Iguchi, M. and Luco, J.E. (1982). "Vibration of flexible plate on viscoelastic medium," *J. Engrg. Mech.*, ASCE, 108(6), 1103-1120.

Kausel, E. (1974). "Forced vibrations of circular foundations on layered media," *Rpt. No. R74-11*, Dept. of Civil Engrg., Massachusetts Inst. Technology.

Kramer, S.L. (1996). *Geotechnical Earthquake Engineering.* Prentice Hall, Upper Saddle River, NJ, pg. 294-303.

Liou, G.-S. and Huang, P.-H. (1994). "Effect of flexibility on impedance functions for circular foundations," *J. Engrg. Mech.*, ASCE, 120(7), 1429-1446.

Roesset, J.M. (1980). "A review of soil-structure interaction," *in* Soil-structure interaction: the status of current analysis methods and research, J.J. Johnson, ed., *Rpt. No. NUREG/CR-1780 and UCRL-53011*, U.S. Nuclear Regulatory Com. and Lawrence Livermore Lab.

Riggs, H.R. and Waas, G. (1985). "Influence of foundation flexibility on soil-structure interaction," *J. Eq. Engrg. Struct. Dynamics*, 13(5), 597-615.

Seed, H.B. (1986). "Influence of local soil conditions on ground motions and building damage during earthquakes," 8th Nabor Carillo Lecture, 13th Nat. Mtg. Of Mexican Society for Soil Mech., Sinaloa, Mexico, November.

Stewart, J.P., Fenves, G.L. and Seed, R.B. (1999a). "Seismic Soil-Structure Interaction in Buildings. I: Analytical Aspects," *J. Geotech.. & Geoenv. Engrg.*, ASCE, 125 (1), 26-37.

Stewart, J.P., Seed, R.B., and Fenves, G.L. (1999b). "Seismic Soil-Structure Interaction in Buildings. II: Empirical Findings," *J. Geotech. & Geoenv. Engrg.*, ASCE, 125 (1), 38-48.

Stewart, J.P. and Fenves, G.L. (1998). "System Identification for Evaluating Soil-Structure Interaction Effects in Buildings from Strong Motion Recordings," *Earthquake Engineering and Structural Dynamics*, 27, 869-885.

Stewart, J.P. (1999). "Variations between foundation-level and free-field earthquake ground motions," *Earthquake Spectra*, EERI (in review).

Veletsos, A.S. and Prasad, A.M. (1989). "Seismic interaction of structures and soils: stochastic approach," *J. Struct. Engrg.*, ASCE, 115(4), 935-956.

Veletsos, A.S., Prasad, A.M., and Wu, W.H. (1997). "Transfer functions for rigid rectangular foundations," *J. Earthquake Engrg. Struct. Dynamics*, 26 (1), 5-17.

Veletsos, A.S. and Nair V.V. (1975). "Seismic interaction of structures on hysteretic foundations," *J. Struct. Engrg.*, ASCE 101(1), 109-129.

Veletsos, A.S. and Verbic, B. (1973). "Vibration of viscoelastic foundations," *J. Eq. Engrg. Struct. Dynamics*, 2(1), 87-102.